HIPPOCAMPUS 25:208–218 (2015)

A Computational Study on Plasticity During Theta Cycles at Schaffer Collateral Synapses on CA1 Pyramidal Cells in the Hippocampus

Ausra Saudargiene,[1]* Stuart Cobb,[2] and Bruce P. Graham[3]

ABSTRACT: Cellular activity in the CA1 area of the hippocampus waxes and wanes at theta frequency (4–8 Hz) during exploratory behavior of rats. Perisomatic inhibition onto pyramidal cells tends to be strongest out of phase with pyramidal cell activity, whereas dendritic inhibition is strongest in phase with pyramidal cell activity. Synaptic plasticity also varies across the theta cycle, from strong long-term potentiation (LTP) to long-term depression (LTD), putatively corresponding to encoding and retrieval phases for information patterns encoded by pyramidal cell activity (Hasselmo et al. (2002a) Neural Comput 14:793–817). The mechanisms underpinning the phasic changes in plasticity are not clear, but it is likely that inhibition plays a role by affecting levels of electrical activity and calcium concentration at synapses. We explore the properties of synaptic plasticity during theta at Schaffer collateral synapses on CA1 pyramidal neurons and the influence of spatially and temporally targeted inhibition using a detailed multicompartmental model of the CA1 pyramidal neuron microcircuit and a phenomenological model of synaptic plasticity. The results suggest CA3-CA1 synapses are potentiated on one phase of theta due to high calcium levels provided by paired weak CA3 and layer III entorhinal cortex (EC) inputs even when somatic spiking is inhibited by perisomatic interneuron activity. Weak CA3 inputs alone induce lower calcium transients and result in depression of the CA3-CA1 synapses. These synapses are depressed if activated in phase with dendritic inhibition as strong CA3 inputs alone are not able to cause high calcium in this theta phase even though the CA1 pyramidal neuron shows somatic spiking. Dendritic inhibition acts as a switch that prevents LTP and promotes LTD during the retrieval phases of the theta rhythm in CA1 pyramidal cell. This may be important for not overly reinforcing recalled memories and in forgetting no longer relevant memories. © 2014 Wiley Periodicals, Inc.

KEY WORDS: spike-timing-dependent plasticity; hippocampus; CA1; inhibitory interneurons; theta oscillations

INTRODUCTION

The variation in synaptic plasticity across 4 to 8 Hz theta cycles in CA1 of rat hippocampus has been proposed to correspond to phases of encoding (propensity for synaptic LTP) and retrieval (propensity for LTD) (Hasselmo et al., 2002a). The functional implications of this hypothesis have been explored in rate-based activity models (Hasselmo et al., 2002a; Judge and Hasselmo, 2004; Zilli and Hasselmo, 2006; Manns et al., 2007) and spiking neural models (Hasselmo et al., 2002b; Cutsuridis et al., 2010) of CA1. These models do not address the underlying network, cellular and synaptic mechanisms that underpin this waxing-and-waning of synaptic plasticity across a theta cycle. Here we use a detailed compartmental model of a CA1 pyramidal cell (PC) to investigate the possible long-term synaptic plasticity outcomes at synapses from CA3 PCs onto the PC during theta activity.

Pyramidal cells in CA1 of the mammalian hippocampus, like pyramidal cells throughout the cortex, receive spatially targeted, temporally patterned excitation, and inhibition. Electrical and chemical activity at individual synapses on such a pyramidal cell will be influenced by coincident excitation and inhibition from other active synapses on the cell. This could result in the plasticity of a synapse being a function not only of presynaptic activity at that synapse, but also the postsynaptic voltage depolarisation at the synapse due to surrounding electrical activity (Graham et al., 2014). For proximal synapses at least, this is evident in the dependence of LTP/LTD on the timing of postsynaptic spikes, relative to presynaptic input. This has been termed spike-timing-dependent plasticity (STDP) (Markram et al., 1997; Bi and Poo, 2001). However, LTP may occur without somatic spiking, with the voltage transient due to local synaptic activity being the determining factor (Golding et al., 2002; Remy and Spruston, 2007; Hardie and Spruston, 2009). Oscillations in recorded local field potentials (LFP) and EEGs are symptomatic of rhythmic variation in synaptic drive to neurons (Brankack et al., 1993). Such rhythmic variation will likely translate into variation in the postsynaptic voltage transients seen by individual synapses and thus a rhythmic variation in the likelihood a synapse will undergo LTP or LTD on arrival of a presynaptic signal. There is experimental evidence for this during active exploration in rats, in which the hippocampus exhibits a pronounced theta rhythm (4–8 Hz) with neuronal population activities being phasic with respect to this rhythm. Schaffer collateral inputs from CA3 PCs to

[1] **Department of Informatics, Vytautas Magnus University, Kaunas, Lithuania;** [2] **Institute of Neuroscience and Psychology, University of Glasgow, Glasgow, Scotland, United Kingdom;** [3] **Computer Science and Mathematics, School of Natural Sciences, University of Stirling, Scotland, United Kingdom.**

Grant sponsor: Research Council of Lithuania; Grant number: MIP-93/2010.

*Correspondence to: Ausra Saudargiene, Department of Informatics, Vytautas Magnus University, Kaunas, LT-44248, Lithuania.
E-mail: a.saudargiene@if.vdu.lt

Accepted for publication 10 September 2014.
DOI 10.1002/hipo.22365
Published online 13 September 2014 in Wiley Online Library (wileyonlinelibrary.com).

the dendrites in stratum radiatum (SR) of CA1 PCs are more likely to undergo LTP if stimulated at the theta peak of the locally recorded LFP (Holscher et al., 1997; Hyman et al., 2003). This corresponds to a period of only weak input from CA3, but strong excitatory input to stratum lacunosum-moleculare (SLM) from entorhinal cortex (EC) layer III cells (Brankack et al., 1993). Subsequently we will refer to this as the encoding phase of theta, in line with the Hasselmo hypothesis (Hasselmo et al., 2002a). Conversely, these synapses may undergo LTD if stimulated on the trough of local theta (Hyman et al., 2003), when CA3 input is actually at its strongest (Brankack et al., 1993). We will refer to this as the retrieval phase of theta (Hasselmo et al., 2002a).

These two opposite phases of theta also correspond to a distinct difference in the pattern of inhibition seen by the CA1 PCs (Klausberger et al., 2003; Klausberger et al., 2004). On the encoding phase a PC is experiencing strong perisomatic inhibition from basket cells (B) and axoaxonic cells (AA), leading to a low probability of spiking, but enabling the dendrites to be depolarised by the combined strong EC and weak CA3 excitatory inputs. On the opposite retrieval phase, when CA3 input is strong, so is dendritic inhibition from bistratified cells (BS) and oriens lacunosum-moleculare (OLM) cells, which may limit long-lasting dendritic depolarisation and thus prevent LTP, while allowing the CA3 input to generate CA1 PC spiking. Similar roles for spatially-targeted inhibition in promoting either encoding or retrieval were proposed by Paulsen and Moser (1998).

Whether the waxing-and-waning of excitatory and inhibitory synaptic activity can directly account for the phasing of synaptic plasticity of the CA3 inputs across a theta cycle, in the manner described above, is as yet hypothetical. We use a detailed compartmental model of a CA1 PC embedded in a CA1 inhibitory microcircuit model to investigate the possible long-term synaptic plasticity outcomes at CA3 pyramidal cell Schaffer collateral synapses onto the CA1 PC in SR during theta activity. Excitatory and inhibitory synapses are distributed in the dendrites of the CA1 PC. CA3 and EC excitatory inputs are modeled by spike trains exhibiting theta burst activity, similar to patterns of in vivo spiking activity and as used in experiments to induce plasticity (Hyman et al., 2003; Judge and Hasselmo, 2004). These trains drive the inhibitory interneurons as well. Synaptic activity causes electrical activity in the receiving PC, mediated by passive and active (sodium, calcium and potassium) currents. It also results in calcium influx, particularly in the spine heads. Spine head calcium is the driving force for intracellular signalling pathways that mediate long-term synaptic plasticity and variation in spine head calcium across a theta cycle may account for the change from LTP to LTD (Hyman et al., 2003). A phenomenological model of synaptic modifications (Graupner and Brunel, 2012) is used to analyze the properties of synaptic plasticity at the CA3-CA1 Schaffer collateral synapses. Simulations of multiple theta cycles are run to establish the plasticity outcome in different circumstances, such as the presence or absence of spatially targeted inhibition (Paulsen and Moser, 1998).

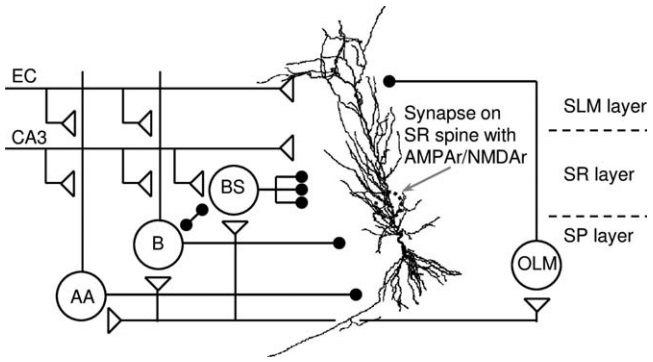

FIGURE 1. Microcircuit of a CA1 pyramidal neuron. Compartmental model of a CA1 pyramidal neuron (Poirazi et al., 2003) with the added AMPA/NMDA synapse on a SR spine, embedded in a microcircuit consisting of oriens lacunosum-moleculare (OLM), bistratified (BS), basket (B), axoaxonic (AA) inhibitory interneurons (Cutsuridis et al., 2010). Synaptic inputs come from entorhinal cortex (EC) and CA3 region. CA1 stratum lacunosum-moleculare (SLM), stratum radiatum (SR) and stratum pyramidale (SP) layers are shown schematically.

Methodology

In this study we embed a well-established, detailed multicompartmental model of a CA1 pyramidal cell (Poirazi et al., 2003) and a calcium-based synaptic plasticity rule (Graupner and Brunel, 2012) into a previously published model of the CA1 microcircuit (Cutsuridis et al., 2010). Thus we replace the simplified PC model and voltage-based plasticity rule used in the original microcircuit model with more physiological counterparts. We retain the excitatory input patterning and the inhibitory interneuron microcircuit that consists of two basket cells, one axoaxonic cell, one bistratified cell, one OLM cell and inputs from the EC and CA3 Schaffer collaterals (Cutsuridis et al., 2010) (Fig. 1). Interneurons have simplified morphologies. Full details of the pyramidal neuron model are given in Poirazi et al. (2003a,b) and for the microcircuit model, including details of the interneuron models, in Cutsuridis et al. (2010).

AMPA synapses are distributed randomly on the SR and SLM dendrites of the CA1 pyramidal neuron. Twenty AMPA synapses on SR dendrites receive inputs from the CA3 Schaffer collaterals, and 20 AMPA synapses on SLM dendrites are activated by the inputs coming from EC. Cyclical changes during theta in the strength of synaptic input from the CA3 Schaffer collateral pathway (Wyble et al., 2000; Molyneaux and Hasselmo, 2002) are modeled as a reduction of the AMPA synaptic weight during theta trough. Twenty-six GABAA and GABAB synapses are located in the SR dendrites and receive inputs from a bistratified cell. Two GABAA and GABAB synapses, activated by the OLM cell, provide inhibition to the SLM dendrites. One GABAA synapse, triggerred by the axoaxonic cell, is placed on the axon of the CA1 pyramidal neuron. The soma of the CA1 pyramidal cell is inhibited by two GABAA synapses, activated by two basket cells.

Bistratified, basket and axoaxonic cells are activated by the CA3 Schaffer collateral synaptic inputs and somatic action

TABLE 1.

Peak Synaptic Conductances (nS)

	Postsynaptic				
Presynaptic	CA1 pyramidal neuron	BSC	B	AA	OLM
CA3	Synapse on a SR spine: 0.05 (NMDA), 1.2 (AMPA, encoding phase), 3 (AMPA, retrieval phase)				
CA3	40 (AMPA, encoding phase), 100 (AMPA, retrieval phase)	1 (AMPA)	0.05 (AMPA)	0.02 (AMPA)	–
EC	80 (AMPA)	–	2.5 (AMPA)	2.5 (AMPA)	–
BSC	4 (GABA-A), 0.1 (GABA-B)	–	10 (GABA-A)	–	–
B	100 (GABA-A)	50 (GABA-A)	–	–	–
AA	40 (GABA-A)	–	–	–	–
OLM	20 (GABA-A), 20 (GABA-B)	–	–	–	–
CA1 pyramidal neuron	–	0.5 (AMPA)	0.5 (AMPA)	1 (AMPA)	1 (AMPA)

Type of the postsynaptic receptor is indicated in parentheses.

potentials of the CA1 pyramidal neuron. Basket and axoaxonic cells receive also EC inputs. Basket and bistratified cells inhibit each other. The OLM cell receives excitatory input from the CA1 pyramidal neuron.

The synaptic parameters are presented in Table 1.

Cell populations in CA3 and EC exhibit gamma frequency (around 40 Hz) activity, with average population activity waxing and waning at the slower theta frequency. EC III theta is largely out of phase with CA3 theta (Mizuseki et al., 2009). We model synaptic input during the theta retrieval phase as being strong CA3 input only, represented by 20 CA3 inputs on two successive gamma cycles. Input on the encoding theta phase consists of strong EC input on two successive gamma cycles in combination with weak CA3 inputs on the same gamma cycles (but delayed by 9 ms on average, modeling the direct versus trisynaptic loop delay (Leung et al., 1995)). These ,,bursts" of two reliable inputs represent the likely synaptic outcome of the theta burst protocol that is commonly required to induce LTP (Hyman et al., 2003). Theta frequency is taken to be 4 Hz, and gamma frequency is 40 Hz.

The combination of excitatory and inhibitory inputs results in the following scenario. The CA1 pyramidal neuron is driven by spatially-focussed patterns of excitation and inhibition depending on the phase of theta. During the encoding phase, EC inputs arrive at the apical SLM dendrites and CA3 inputs arrive at SR dendrites. EC inputs are strong enough to induce local dendritic spikes and cause somatic spiking whereas CA3 inputs are weak in this phase. However, AA and B interneurons receive activation from EC and CA3 inputs and inhibit the axon and soma of the pyramidal neuron preventing its spiking. During the retrieval phase, EC inputs are weak or absent and CA3 inputs are strong to induce somatic spiking as AA and B cells are inactive. The apical dendrites are inhibited by BS and OLM cells in this phase.

Synaptic plasticity is examined in a single spine of the CA1 pyramidal cell. This spine is formed on the medial SR apical dendrite (144 μm from the soma) and has AMPA and NMDA receptor-gated channels. Spine head diameter and length equal 0.5 μm, spine neck diameter is 0.2 μm and length 1 μm. NMDA synaptic conductance is 0.05 nS. AMPA synaptic conductance is 3 nS if a synapse is activated on the retrieval phase, and reduced to 1.2 nS, if it is activated on the encoding phase, this way capturing the suppression of the strength of synaptic transmission.

Note that the bulk excitatory input from CA3 and EC (not including the spine) is, for computational efficiency, to synapses on dendritic shafts, with conductances suitably scaled to achieve the desired somatic and dendritic spiking activity. Twenty inputs are sufficient to give a broad depolarisation of the dendrites without having to model a larger population of inputs.

Calcium concentration in a spine is modeled as influx through NMDA and voltage-gated calcium channels, with extrusion via pumps and buffers accounted for with a single decay time constant (Badoual et al., 2006).

The calcium-based, phenomenological Graupner-Brunel model of synaptic plasticity (Graupner and Brunel, 2012) is applied to determine synaptic modifications in the SR spine. Changes in synaptic weight are represented by the state transitions of the synaptic efficacy variable ρ and are driven by the intracellular calcium concentration in the spine. Synaptic efficacy variable ρ describes the competition of kinases and phosphotases in an abstract way and represents a model of the binary synapse. ρ can reside in two stable states, so-called DOWN and UP states. Transition from the DOWN state to the UP state is triggered by high intracellular calcium concentration levels and is considered as potentiation of the synapse. Transition from the UP state to the DOWN state is induced

TABLE 2.

Parameters of the STDP Model

Parameter	Value	Description and units
θ_d	1	LTD threshold
θ_p	1.3	LTP threshold
γ_d	300	Rate of decrease in ρ
γ_p	1,600	Rate of increase in ρ
τ	100	Time constant of ρ changes; s
ρ_*	0.5	Unstable ρ state

by low prolonged calcium signals and is regarded as depression of the synapse.

Synaptic efficacy variable ρ is described by a first-order differential equation (Graupner and Brunel, 2012):

$$\tau\frac{d\rho}{dt} = -\rho(1-\rho)(\rho_*-\rho)+\gamma_p(1-\rho)\Theta[c(t)-\theta_p] -\gamma_d\rho\Theta[c(t)-\theta_d]+Noise(t) \quad (1)$$

where $c(t)$ is the instantaneous calcium concentration, Θ denotes the Heaviside function, and all the remaining parameters and their values are presented in Table 2. Noise term $Noise(t)$ is not implemented.

Synaptic changes during theta cycles are modeled to reveal the influence of temporal patterns of EC and CA3 inputs and activity of inhibitory cells on synaptic modifications at Schaffer collateral synapses in a hippocampal CA1 pyramidal neuron. The intracellular calcium concentration in the SR spine during synaptic activity is determined and the resulting synaptic efficacy ρ is computed over time. Initially, ρ is set to the DOWN or to the UP state, to represent either an initially unpotentiated or a potentiated synapse. Transitions from the DOWN to the UP or from the UP to the DOWN states are regarded as changes in synaptic weight.

The numerical simulations were performed using NEURON (Hines and Carnevale, 1997) running on a PC under Windows XP. The code is adapted from the publically-available code on ModelDB (https://senselab.med.yale.edu/ModelDB/) for the Poirazi CA1 pyramidal cell (ModelDB accession number 20212) and the Cutsuridis microcircuit model (ModelDB accession number 123815) and is available as ModelDB accession number 157157.

In the simulations, theta-modulated inputs from CA3 and EC were applied in a consistent pattern for 16 theta cycles. During these cycles, the inputs to the CA3 synapse on the SR spine were applied either during the encoding or retrieval phase of theta, depending on the experiment being performed. The following simulation protocols of the pyramidal neuron were applied, based on the encoding/retrieval hypothesis (Hasselmo et al., 2002a; Cutsuridis et al., 2010):

1. Weak CA3 inputs and EC inputs in encoding phase, strong CA3 inputs in retrieval phase; Schaffer collateral synapse (on SR spine) active in encoding phase. This is a full implementation of the hypothesised encoding phase.
2. Weak CA3 inputs and EC inputs in encoding phase, strong CA3 inputs in retrieval phase; Schaffer collateral synapse is active in retrieval phase. This is a full implementation of the hypothesised retrieval phase.
3. Weak CA3 inputs in encoding phase, strong CA3 inputs in retrieval phase; Schaffer collateral synapse is active in encoding phase.
4. Weak CA3 inputs without B/AA inhibition in encoding phase, strong CA3 inputs in retrieval phase; Schaffer collateral synapse is active in encoding phase.
5. Strong CA3 inputs in encoding phase, strong CA3 inputs in retrieval phase; Schaffer collateral synapse is active in encoding phase.
6. Weak CA3 inputs and EC inputs in encoding phase, strong CA3 inputs without BS inhibition in retrieval phase; Schaffer collateral synapse is active in retrieval phase.

RESULTS

The first simulation protocol is a full implementation of the hypothesised encoding phase of theta. Figure 2 shows somatic and dendritic membrane potentials, SR spine head calcium concentration, the induced transitions of the synaptic efficacy variable ρ in the spine and the raster plots of the CA3 and EC inputs for 16 theta cycles (4 s) of the first stimulation protocol. In the encoding phases (0–0.125 s, 0.250–0.375 s, 0.500–0.625 s, 0.750–0.875 s, 1.000–1.125 s, etc.) the Schaffer collateral pathway on the SR spine is active and weak CA3 inputs (Fig. 2f, gray dots) are paired with the EC inputs (Fig. 2e) and induce dendritic spikes (Fig. 2b). However, perisomatic inhibition provided by AA and basket interneurons prevents somatic spiking during this phase (Fig. 2a). Activation of NMDAr on the SR spine, paired with the strong postsynaptic depolarisation, produces high prolonged calcium transients during the encoding phases, rising up to 1.6 μM (Fig. 2c). In the retrieval phases (0.125–0.250 s, 0.375–0.500 s, 0.625–0.500 s, 0.875–1 s, 1.125–1.250 s, etc.), EC inputs are absent but strong CA3 inputs (Fig. 2f, black dots) alone are sufficient to induce somatic spiking (Fig. 2a). Calcium levels in the SR spine do not reach the heights of the encoding phases (Fig. 2c) as the SR dendritic region is inhibited by bistratified interneurons, and in addition, spine NMDAr are almost closed as no additional spine inputs are assumed during this retrieval phase.

The high calcium transients in the SR spine during the encoding phase, induced by the combined CA3 and EC inputs, lead to a transition of the synaptic efficacy variable ρ from the DOWN state to the UP state (Fig. 2d, solid line) and prevent its transition from the UP state to the DOWN state (Fig. 2d, dotted line). So an unpotentiated synapse will undergo LTP induction, and an already potentiated synapse will remain so. Thus the PC's association with this CA3 input will be increased due to its co-occurrence with the EC inputs, as per the hypothesis.

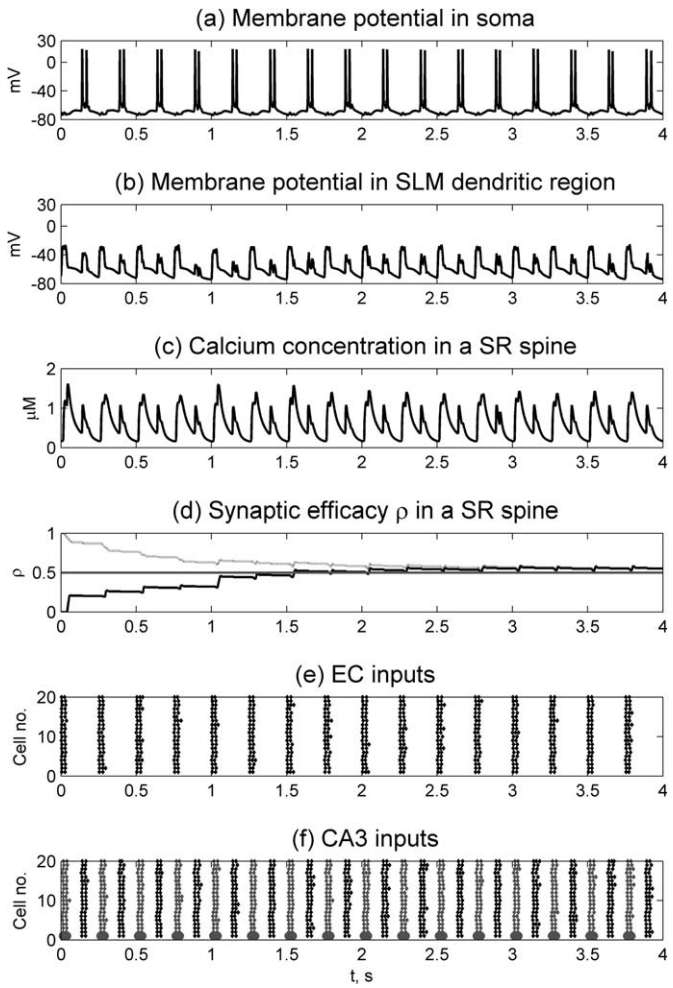

FIGURE 2. Regional membrane potential and spine calcium concentration in CA1 PC for simulation protocol 1. (a) Membrane potential in soma. (b) Membrane potential in SLM dendritic region. (c) Calcium concentration in exemplar SR spine. (d) Synaptic efficacy ρ in SR spine (initially in DOWN state—solid line; initially in UP state—dotted line); LTP is induced. (e) Raster plot of 20 EC inputs, active on encoding phase. (f) Raster plot of 20 CA3 inputs (weak inputs on encoding phase—gray dots, strong inputs on retrieval phase—black dots). Schaffer collateral pathway on exemplar SR spine is weakly active on theta encoding phase (large gray circles at bottom of raster plot of CA3 inputs, (f)).

The second simulation protocol is a full implementation of the hypothesised retrieval phase, and the results are presented in Figure 3. The Schaffer collateral pathway on the test SR spine is now active on the retrieval phase. In the encoding phase, weak CA3 inputs are again paired with the EC inputs (Figs. 3e,f, gray dots) and induce dendritic spikes (Fig. 3b). However, as there is no synaptic input to the spine on this phase, calcium currents are mediated by voltage-sensitive calcium channels (VSCC) alone, as the NMDAr are closed. Therefore spine calcium levels remain low, ~0.9 μM (Fig. 3c). Somatic spiking is prevented by perisomatic inhibition (Fig. 3a).

In the retrieval phase, strong CA3 inputs (Fig. 3f, black dots) again cause somatic spiking (Fig. 3a). Although the SR spine is depolarised by the back-propagating spike and the synapse on this SR spine is activated (NMDAr are open), the resulting calcium concentration typically rises only slightly above 1.1 μM as the SR dendritic region is inhibited by bistratified interneurons and the EC inputs are silent. In addition, the SLM dendritic region is inhibited by OLM cells.

The low calcium concentrations seen by the SR spine during this protocol provoke the transition of the synaptic efficacy variable ρ from the UP state to the DOWN state (Fig. 3d, dotted line), but are not sufficient to cause transition from the DOWN state to the UP state (Fig. 3d, solid line), and thus LTD induction is promoted, particularly during the retrieval phase. Note that the spine head calcium does breach the LTP threshold (set at 1.3 μM) a couple of times (at around 3 s in

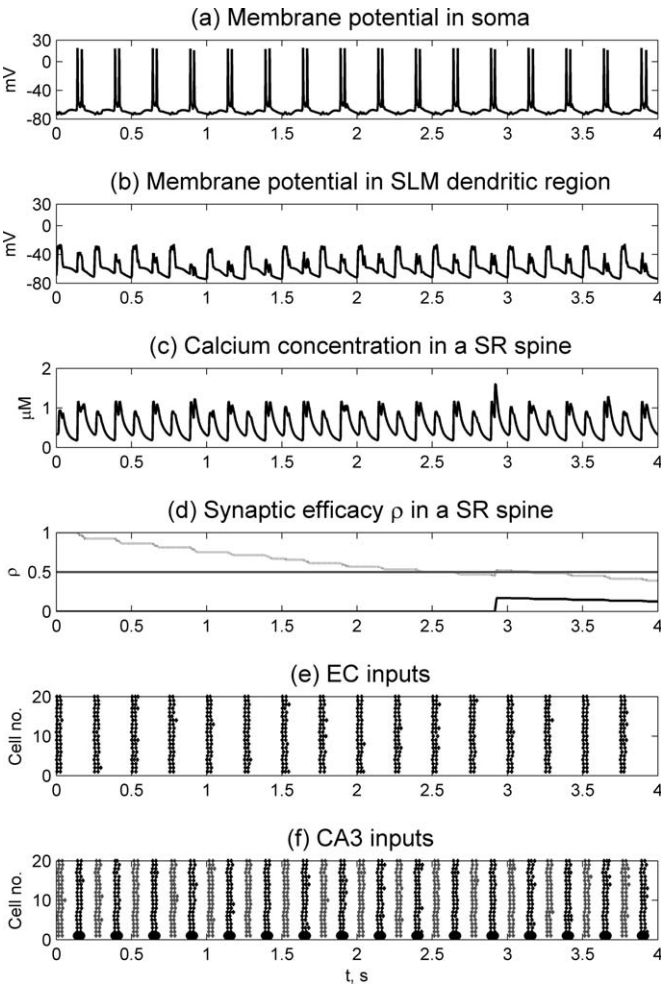

FIGURE 3. Regional membrane potential and spine calcium concentration in CA1 PC for simulation protocol 2. (a) Membrane potential in soma. (b) Membrane potential in SLM dendritic region. (c) Calcium concentration in exemplar SR spine. (d) Synaptic efficacy ρ in SR spine (initially in DOWN state—solid line; initially in UP state—dotted line); LTD is induced. (e) Raster plot of 20 EC inputs, active on encoding phase. (f) Raster plot of 20 CA3 inputs (weak inputs on encoding phase—gray dots, strong inputs on retrieval phase—black dots). Schaffer collateral pathway on exemplar SR spine is strongly active on theta retrieval phase (large black circles at bottom of raster plot of CA3 inputs, (f)).

this simulation) and so ρ starting in the DOWN state does increase, but does not get near the level required to trigger LTP. SR activity contributes to CA1 PC spiking, and thus retrieval of previously encoded inputs, but may be subject to depression if not reinforced during subsequent encoding phases, leading to reversal of prior learning, as per the hypothesis and model of Hasselmo (Hasselmo, 2002a).

The remaining four simulation protocols explore the consequences of blocking inhibition or changing excitatory input strengths, in either of the encoding or retrieval phases. The results, along with the first two protocols, are presented together in Figures 4 and 5. For clarity in Figure 4, traces of key variables from a single theta cycle are shown. The first half of the theta cycle is the encoding phase and the second half is the retrieval phase. In Figure 5, the synaptic efficacy ρ, is shown over the course of an entire 4 s simulation, as it changes slowly.

The third simulation protocol is the same as the first, except that the EC input is absent so that only the weak CA3 inputs alone (Figs. 4c and 5c) excite the pyramidal neuron in the encoding phase. In the encoding scenario, this corresponds to a pattern of inputs to a pyramidal cell that should not become associated with the current CA3 inputs (Cutsuridis et al., 2010). Without EC-induced dendritic spikes the SR spine is only moderately depolarised and consequently spine calcium levels are lower, around 1.3 μM (Fig. 4c3). Somatic spiking is not observed during this phase due to perisomatic inhibition (Fig. 4c1). In the retrieval phase, strong CA3 inputs still induce somatic spiking, but again, as in the first protocol, calcium levels do not increase substantially.

Now the lower calcium signal in the SR spine results in the transition of the synaptic efficacy variable ρ from the UP state to the DOWN state (Fig. 5c), and prevents transition from the DOWN state to the UP state (Fig. 5c). The spine head calcium does occasionally breach the LTP threshold (set at 1.3 μM) and so ρ starting in the DOWN state does increase, but not sufficiently to trigger LTP. So a potentiated synapse will now be depressed (LTD) and an unpotentiated synapse will remain so. Thus, in accord with the hypothesis, the association with this CA3 input will be unchanged or decreased ("forgotten").

These outcomes depend on the combination of weakened CA3 inputs and the presence of perisomatic B/AA inhibition. Figures 4d and 5d show that the removal of the B/AA inhibition allows LTP of the weak CA3 inputs even in the absence of coincident EC input. These weak CA3 inputs are still sufficient to induce somatic spiking when perisomatic inhibition is absent (Fig. 4d1, with the consequent back-propagating action potentials resulting in significant calcium transients in the active SR spine head (Fig. 4d3). Also, strong CA3 inputs alone, even with B/AA inhibition, can induce large enough calcium transients (Fig. 4e3) that LTP occurs at the SR spine head synapse (Fig. 5e).

Figures 4f and 5f present the results of the sixth simulation protocol. Dendritic inhibition provided by bistratified interneurons is now removed from the retrieval phase to assess its impact. The strong CA3 inputs on the retrieval phase now cause bursts of somatic action potentials (Fig. 4f1). With the Schaffer collateral pathway on the SR spine active during the retrieval phase the resulting calcium concentration is high, reaching 40 μM (Fig. 4f3). Synaptic efficacy variable ρ undergoes transition from the DOWN to the UP state (Fig. 5f) or stays in the UP state (Fig. 5f), effectively inducing LTP. This demonstrates the importance of dendritic inhibition in controlling synaptic plasticity and limiting CA1 PC spiking during the retrieval phase.

For all the simulation protocols, peak spine head calcium (Fig. 4, column 3) always occurs when the associated SR synapse is active, which may be either on the encoding or retrieval phase, depending on the protocol. However, there is also calcium entry on the opposite phase through VGCCs. Calcium levels are between 1 and 2 μM when inhibition is intact (Figs. 4a–c) but increase dramatically if dendritic or perisomatic inhibition is removed (Figs. 4d,f) or the SR input synapse is strengthened (Fig. 4e).

In the Graupner-Brunel plasticity model (Graupner and Brunel, 2012), LTD induction begins when the peak calcium passes 1.0 μM and LTP induction when peak calcium is greater than 1.3 μM. The overall time course of LTD/LTP induction depends on the time that spine head calcium spends above the LTD/LTP thresholds, which in turn depends on the individual synaptic stimulus and the number and frequency of repetitions of the stimulus. This is evident in the traces of the synaptic efficacy variable ρ from each protocol, shown in Figure 5. Large calcium peaks result in rapid induction of LTP (Figs. 5d–f), possibly after a single theta cycle. More modest calcium, as achieved in the full encoding phase with inhibition intact, requires around 8 theta cycles for LTP (Fig. 5a). LTD induction requires many more stimulus presentations, around 14 theta cycles at least (Figs. 5b,c).

In summary, these simulation results demonstrate that in the encoding phase of a theta cycle, EC input-induced dendritic spikes may propagate from the SLM dendrites to the SR dendritic regions in the CA1 pyramidal cell, coincide with the (weak) CA3 inputs, induce large calcium influx into the spine on the SR dendrite and cause LTP. In the retrieval phase, dendritic inhibition provided by BS and OLM cells may prevent dendritic spike generation in the SR region, restrict calcium increase and result in LTD of the SR spine synapse. Removing dendritic inhibition in retrieval phases allows generation of dendritic spikes in SR dendrites and converts LTD to LTP.

DISCUSSION

The computer simulations presented here lend credence to the suggestion that fluctuating spine head calcium levels (Hyman et al., 2003) resulting from phasic variation in spatiotemporal excitatory and inhibitory inputs onto a CA1

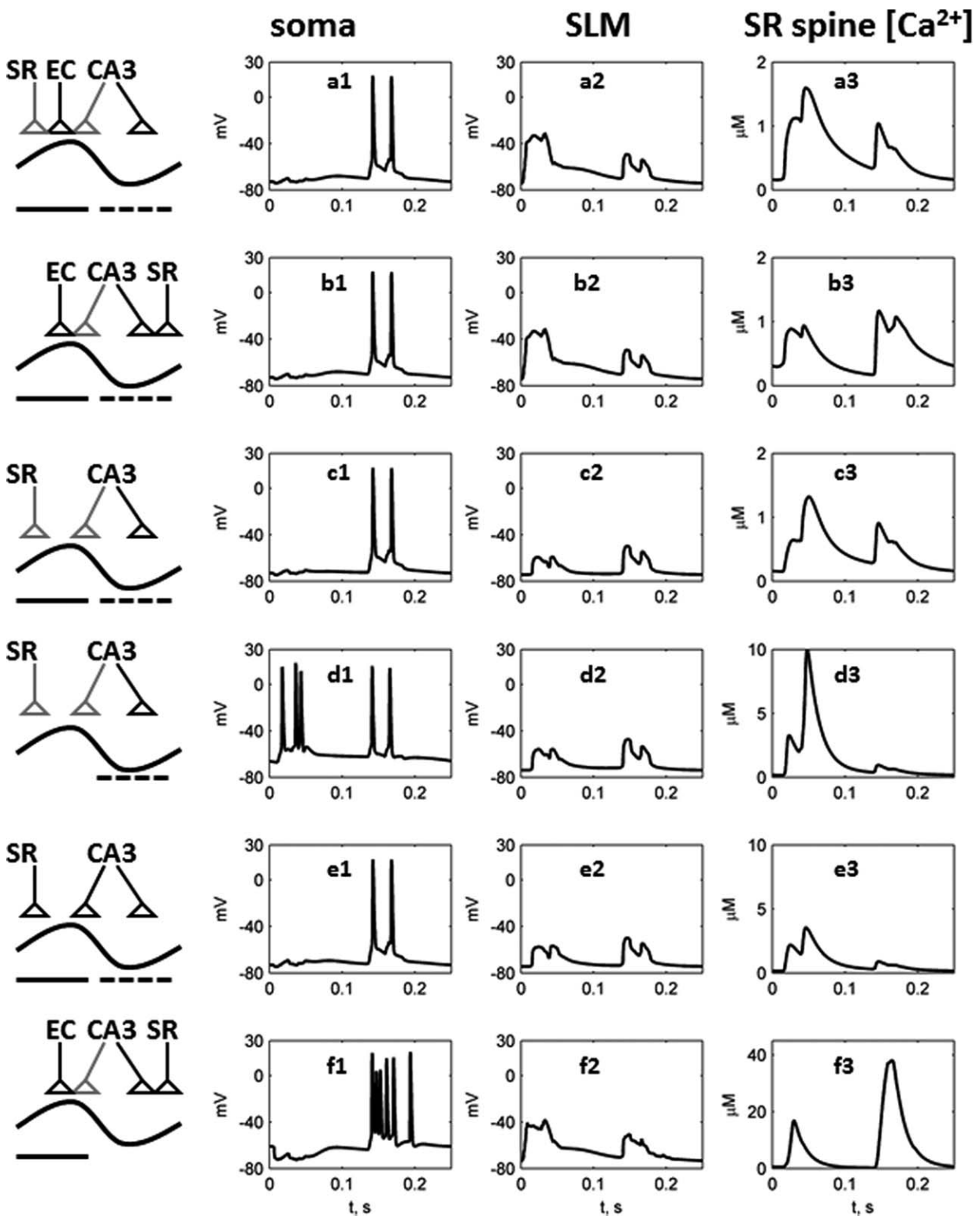

FIGURE 4. Regional membrane potential and spine calcium concentration in CA1 PC from a single theta cycle for all six simulation protocols (rows a–f). Left-hand side: schematics of each protocol—triangles indicate which theta half-cycle the EC, CA3 and exemplar SR spine inputs are active, with first half-cycle being the encoding phase and second half-cycle is the retrieval phase (gray indicates weak input); solid horizontal line indicates presence of perisomatic inhibition and dashed horizontal line is dendritic inhibition. Columns: (a) membrane potential in soma, (b) membrane potential in SLM dendritic region, (c) calcium concentration in exemplar SR spine.

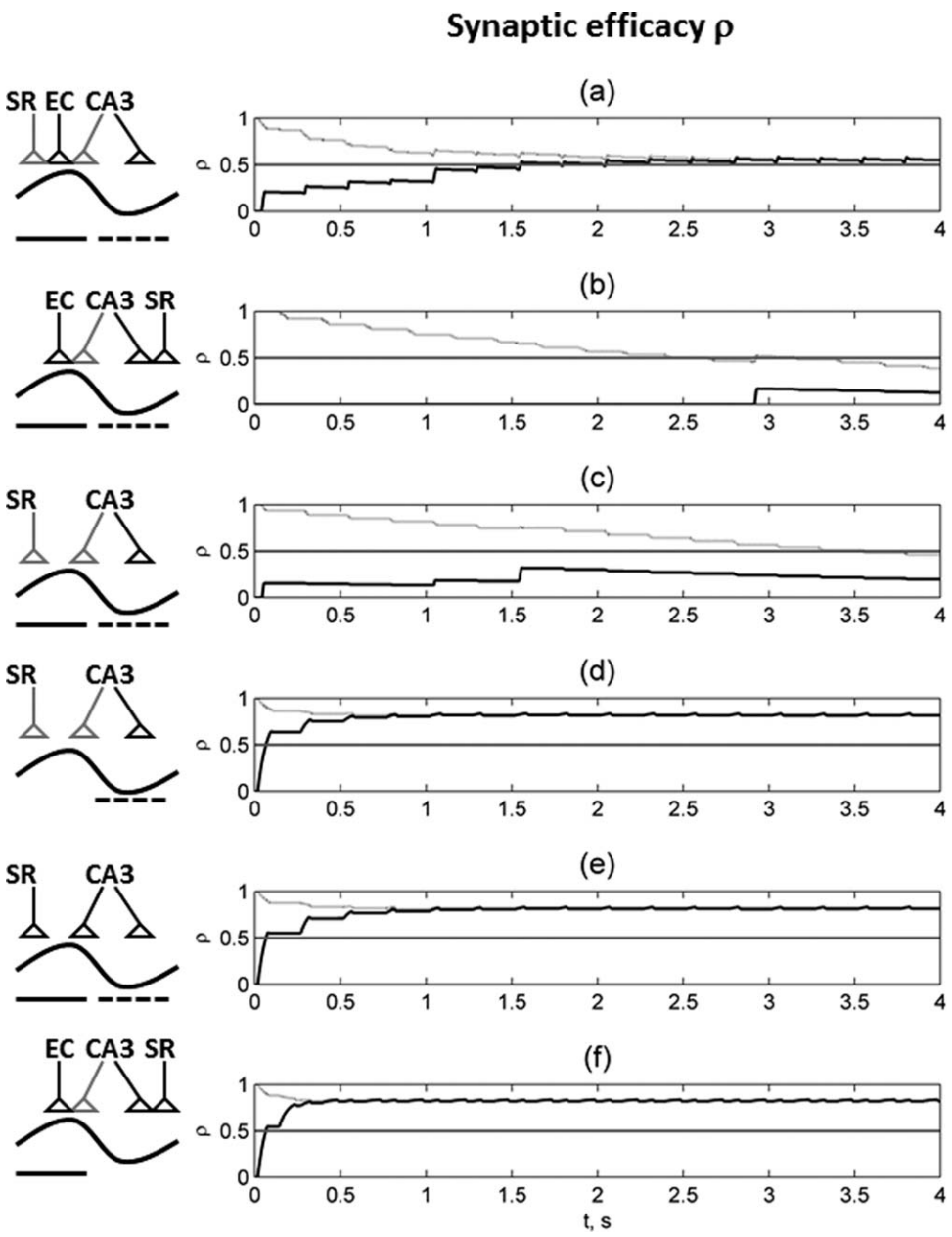

FIGURE 5. Synaptic efficacy ρ in exemplar SR spine (initially in DOWN state—solid line; initially in UP state—dotted line) over full simulation period for all six protocols (a–f). Left-hand side: schematics for each protocol, as for Figure 4.

pyramidal cell lead to theta activity cycles being divided into an encoding phase, during which LTP predominates, and a retrieval phase in which LTD may occur (Hasselmo et al., 2002a). The modeling study predicts the following:

1. Weak CA3 inputs paired with the EC inputs evoke large long-lasting calcium transients and result in potentiation of activated CA3-CA1 synapses even when somatic spiking is inhibited by perisomatic basket cell activity. This corresponds to the hypothesis of LTP on an encoding phase of theta.
2. Weak CA3 inputs alone induce lower calcium transients and result in depression of activated CA3-CA1 synapses when somatic spiking is inhibited by perisomatic basket cell signals. This emphasises the role of the excitatory EC input in inducing LTP at the CA3 Schaffer collateral synapses.
3. During the retrieval theta phase, strong CA3 inputs alone are not able to cause a high calcium increase due to dendritic inhibition provided by bistratified neurons, even though the CA1 pyramidal neuron shows somatic spiking. Consequently the CA3-CA1 synapses become depressed, in line with the hypothesis of LTD on the retrieval phase.

4. Removing dendritic inhibition converts this CA3 input-induced depression on the retrieval phase into potentiation, emphasising the role of spatially-targeted inhibition in the plasticity outcome.

Experimental evidence points to a waxing-and-waning of the ability of Schaffer collateral inputs from CA3 pyramidal cells onto CA1 pyramidal cells in the rat hippocampus to undergo LTP during theta oscillatory activity associated with active exploration (Holscher et al., 1997; Hyman et al., 2003; Judge and Hasselmo, 2004). In agreement with the experimental data, such a synapse is able to undergo LTP if it is activated during the half-theta cycle in which inputs from EC are strong, but Schaffer collateral inputs are weak. Somatic spiking is not required, and is unlikely due to strong perisomatic inhibition. Without the coincident EC inputs, no change or LTD is most likely at these SR synapses. On the other theta half-cycle, inputs from CA3 are strong, but due to coincident dendritic inhibition mediated by bistratified cells, the SR synapses are likely to experience no change or LTD, even though the Schaffer collateral input is sufficient to produce spiking in the CA1 pyramidal cell. In summary, our computational model indicates that the local calcium transients at individual SR synapses vary across a theta cycle due to phasic oscillations in the excitatory and inhibitory inputs to the pyramidal cell, making LTP likely on one half-cycle and no change or LTD likely on the opposite half-cycle.

The model highlights the crucial role of perisomatic and dendritic inhibition in these outcomes (Paulsen and Moser, 1998). The different impact of these two distinct forms of inhibition on spine head calcium transients during a single burst input to an SR spine was demonstrated in Graham and Spera (2014), but this was not related directly to a plasticity outcome nor to continuous phasic inputs during multiple theta cycles. Though inhibitory interneurons can be broadly classified as perisomatic- or dendrite-targeting (Bartos et al., 2010), spatio-temporal inhibition in the CA1 hippocampus is far more complex than this, with many different cell classes contributing to rhythmic PC activity and likely to PC synaptic plasticity in different behavioral conditions (Somogyi and Klausberger, 2005). Computational modeling will be key to untangling the functional contribution of further classes of inhibitory interneurons (Cutsuridis and Hasselmo, 2012; Bezaire and Soltesz, 2013).

A physiologically reasonable instantiation of the Hasselmo hypothesis (Hasselmo et al., 2002a) has not previously been modeled. Encoding and retrieval of PC activity patterns on separate theta phases has been demonstrated in a spiking neural network model (Cutsuridis et al., 2010). However, learning in this model was greatly simplified as being driven by a single voltage threshold in the SR dendrites and could only occur during the encoding phase i.e. synaptic plasticity was switched off during the retrieval phase. Thus associations could be encoded and retrieved, but not erased by LTD during the retrieval phase, in this model. An updated version of this network model uses a calcium-based plasticity model, but this is driven by a bulk dendritic calcium signal in a PC model with simplified morphology, and the variation in plasticity over a theta cycle is not investigated (Cutsuridis and Hasselmo, 2012). Here we have used a biophysically-based model of LTP and LTD induction, involving the calcium transients induced in a single synaptic spine head during temporally and spatially distributed synapse input across morphologically realistic dendrites. The plasticity induction process is fully available at a synapse throughout theta and so the plasticity outcome on opposite phases of theta entirely depends on phasic synaptic activity during theta and the associated variation in spine head calcium levels.

The functional implications of this theta-phasic synaptic plasticity have been explored in a number of computational models by Hasselmo and colleagues (Hasselmo et al., 2002a,b; Judge and Hasselmo, 2004; Zilli and Hasselmo, 2006; Manns et al., 2007). Temporal separation of the encoding of new information from the retrieval of old information reduces interference from the retrieval of already stored patterns during the encoding process. Such interference could lead to distorted and incorrect associations between sensory (event) and contextual information being stored. Possible LTD on the phase when pattern retrieval is prominent can allow the forgetting of stored information that is no longer relevant. A stored association that is still relevant will be present in synaptic input throughout theta, and its reencoding (LTP) will be balanced by forgetting (LTD), whereas if the environment changes so that an encoding context provided by EC input is not present, the association will only be subject to LTD during the retrieval phase and will fade away (Hasselmo et al., 2002a).

Not only is plasticity a function of recent synaptic activity, our model also demonstrates that the outcome of LTP or LTD depends on the repetition of particular patterns of synaptic activity over many theta cycles, with LTP induction occurring faster than LTD (Fig. 5). This is in line with experimental results (Wittenberg and Wang, 2006) as modeled by Graupner and Brunel (2012). This implies that a short, but significantly novel stimulus will be remembered, whereas forgetting of old stimuli is rather conservative, requiring retrieval of the old stimulus without reinforcement by a relevant contextual signal (Hasselmo et al., 2002a) for a longer period before LTD is invoked. This would seem to be behaviorally reasonable, as significant new events may be quite brief, whereas stored episodic memories should only be erased if it is certain that they are no longer relevant to current behavior. We refer here only to hippocampus-dependent learning and forgetting of declarative / episodic memories during ongoing behavior, though similar considerations may apply to all activity patterns in the brain, including long-term memories in neocortex.

Our results highlight the key role that spatially and temporally targeted inhibition may play in the promotion of LTP and LTD on separate phases of a theta cycle. If it was possible experimentally to selectively block perisomatic basket cell and dendritic bistratified cell inhibition, for example, by optogenetic suppression, then the model predicts that experiments in awake, behaving animals, such as performed by Hyman et al.

(2003), should reveal the following. First, blocking of EC input to CA1, with inhibition intact, should result in LTD only occurring throughout theta and a consequent loss of the ability to form new episodic memories. Blockade of perisomatic inhibition, with EC input still blocked, could restore LTP on the encoding phase. This has the behavioral consequence that associations will be formed with all activity from CA3, whether or not it is associated with a novel stimulus highlighted by a "context" signal from EC. With the EC input and perisomatic inhibition intact, but with dendritic bistratified cell inhibition blocked, only LTP should be seen throughout theta. This should result in the loss of the ability to reverse no longer relevant prior learning and allow the formation of incorrect associations between a current context and old memories (Hasselmo et al., 2002a,b).

Cellular spiking activity is also phasic over theta in pyramidal cells and different classes of inhibitory interneurons (Klausberger et al., 2003, 2004; Mizuseki et al., 2009). Though we have concentrated solely on the effects of these phasic activity patterns on synaptic plasticity, they also have implications for the spiking output of the CA1 pyramidal cells. We see CA1 spiking largely coincident with strong CA3 inputs. This could be the case for a subset of strongly driven CA1 PCs (Mizuseki et al., 2009), but the spiking activity of the population of CA1 PCs is more complex, with most spiking occurring sometime between the peak of the EC inputs and the CA3 inputs (Manns et al., 2007; Mizuseki et al., 2009). Such phasing is not the result of simple integration of excitatory inputs, but must result from the timed combinations of all excitatory and inhibitory inputs that are varying over the theta cycle (Mizuseki et al., 2009). A complex network model with populations of interneurons providing appropriate feedforward and feedback excitation and inhibition is needed to explore this (Bezaire and Soltesz, 2013). Such a model could provide a more physiological basis for the variation of CA1 spiking phase with the novelty or familiarity of inputs (Manns et al., 2007), in support of the rate-based model of Zilli and Hasselmo (2006).

REFERENCES

Badoual M, Zou Q, Davison AP, Rudolph M, Bal T, Frégnac Y, Destexhe A. 2006. Biophysical and phenomenological models of multiple spike interactions in spike-timing dependent plasticity. Int J Neural Syst 16:79–97.

Bartos M, Sauer J-F, Vida I, Kulik A. 2010. Fast and slow GABAergic transmission in hippocampal circuits. In: Cutsuridis V, Graham B, Cobb S, Vida I, editors. Hippocampal Microcircuits. New York: Springer. Series in Computational Neuroscience, Vol. 5. pp 129–162.

Bezaire MJ, Soltesz I. 2013. Quantitative assessment of CA1 local circuits: Knowledge base for interneuron-pyramidal cell connectivity. Hippocampus 23:751–785.

Bi G, Poo M. 2001. Synaptic modification by correlated activity: Hebb's postulate revisited. Annu Rev Neurosci 24:139–166.

Brankack J, Stewart M, Fox S. 1993. Current source density analysis of the hippocampal theta rhythm: associated sustained potentials and candidate synaptic generators. Brain Res 310–327.

Cutsuridis V, Cobb S, Graham BP. 2010. Encoding and retrieval in a model of the hippocampal CA1 microcircuit. Hippocampus 20: 423–446.

Cutsuridis V, Hasselmo, M. 2012. GABAergic contributions to gating, timing, and phase precession of hippocampal neuronal activity during theta oscillations. Hippocampus 22:1597–1621.

Dudman JT, Tsay D, Siegelbaum SA. 2007. A role for synaptic inputs at distal dendrites: Instructive signals for hippocampal long-term plasticity. Neuron 56:866–79.

Golding NL, Staff NP, Spruston N. 2002. Dendritic spikes as a mechanism for cooperative long-term potentiation. Nature 418:326–31.

Graham BP, Saudargiene A, Cobb S. Spine head calcium as a measure of summed postsynaptic activity for driving synaptic plasticity. Neural Comput 26:2194–2222.

Graham BP, Spera, E. 2014. On phasic inhibition during hippocampal theta. Network 25:3–19.

Graupner M, Brunel N. 2012. Calcium-based plasticity model explains sensitivity of synaptic changes to spike pattern, rate, and dendritic location. Proc Natl Acad Sci USA 109:3991–3996.

Hardie J, Spruston N. 2009. Synaptic depolarization is more effective than back-propagating action potentials during induction of associative long-term potentiation in hippocampal pyramidal neurons. J Neurosci 29:3233–3241.

Hasselmo M, Bodelon C, Wyble B. 2002a. A proposed function of the hippocampal theta rhythm: separate phases of encoding and retrieval of prior learning. Neural Comput 14:793–817.

Hasselmo ME, Hay J, Ilyn M, Gorchetchnikov A. 2002b. Neuromodulation, theta rhythm and rat spatial navigation. Neural Networks 15:689–707.

Hines ML, Carnevale NT. 1997. The neuron simulation environment. Neural Comput 9:1179–1209.

Holscher C, McGlinchey L, Anwyl R, Rowan MJ. 1997. HFS-induced long-term potentiation and LFS-induced depotentiation in area CA1 of the hippocampus are not good models for learning. Psychopharmacology (Berl) 130:174–182.

Hyman JM, Wyble BP, Goyal V, Rossi CA, Hasselmo ME. 2003. Stimulation in hippocampal region CA1 in behaving rates yields long-term potentiation when delivered to the peak of theta and long-term depression when delivered to the trough. J Neurosci 23:11725–11731.

Judge SJ, Hasselmo ME. 2004. Theta rhythmic stimulation of stratum lacunosum-moleculare in rat hippocampus contributes to associative LTP at a phase offset in stratum radiatum. J Neurophysiol 92: 1615–1624.

Klausberger T, Magill PJ, Marton LF, David J, Roberts B, Cobden PM, Buzsaki G, Somogyi P. 2003. Brain-state and cell-type-specific firing of hippocampal interneurons in vivo. Nature 421:844–848.

Klausberger T, Marton LF, Baude A, Roberts JD, Magill PJ, Somogyi P. 2004. Spike timing of dendrite-targeting bistratified cells during hippocampal network oscillations in vivo. Nat Neurosci 7:41–47.

Leung LS, Roth L, Canning KJ. 1995. Entorhinal inputs to hippocampal CA1 and dentate gyrus in the rat: A current-source-density study. J Neurophysiol 73:2392–2403.

Manns JR, Zilli EA, Ong, KC, Hasselmo ME, Eichenbaum H. 2007. Hippocampal CA1 spiking during encoding and retrieval: Relation to theta phase. Neurobiol Learn Mem 87:9–20.

Markram H, Lübke J, Frotscher M, Sakmann B. 1997. Regulation of synaptic efficacy by coincidence of postsynaptic APs and EPSPs. Science 275:213–215.

Mizuseki K, Sirota A, Pastalkova E, Buzsaki G. 2009. Theta oscillations provide temporal windows for local circuit computation in the entorhinal-hippocampal loop. Neuron 64:267–280.

Molyneaux BJ, Hasselmo ME. 2002. GABAB presynaptic inhibition has an in vivo time constant sufficiently rapid to allow modulation at theta frequency. J Neurophysiol 87:1196–1205.

Poirazi P, Brannon T, Mel BW. 2003a. Arithmetic of subthreshold synaptic summation in a model CA1 pyramidal cell. Neuron 37: 977–987.

Poirazi P, Brannon T, Mel BW. 2003b. Online supplement: About the model neuron 37 online. 1–20.

Paulsen O, Moser EI. 1998. A model of hippocampal memory encoding and retrieval: GABAergic control of synaptic plasticity. TINS 21:273–278.

Remy S, Spruston N. 2007. Dendritic spikes induce single-burst long-term potentiation. Proc Natl Acad Sci USA 104:17192–17197.

Somogyi P, Klausberger T. 2005. Defined types of cortical interneurone structure space and spike timing in the hippocampus. J Physiol 562.1:9–26.

Wittenberg GM, Wang SS. 2006. Malleability of spike-timing-dependent plasticity at the CA3–CA1 synapse. J Neurosci 26: 6610–6617.

Wyble BP, Linster C, Hasselmo, ME. 2000. Size of CA1-evoked synaptic potentials is related to theta rhythm phase in rat hippocampus. J Neurophysiol 83:2138–2144.

Zilli EA, Hasselmo ME. 2006. An analysis of the mean theta phase of population activity in a model of hippocampal region CA1. Network 7:277–297.